ELSEVIER

Immobilization of nanoparticles by occlusion into microbial calcite

Rebecca L. Skuce [a], Dominique J. Tobler [a,b], Ian MacLaren [c], Martin R. Lee [a], Vernon R. Phoenix [d,*]

[a] School of Geographical & Earth Sciences, Gregory Building, University of Glasgow, G12 8QQ, UK
[b] Nano-Science Center, Department of Chemistry, University of Copenhagen, Universitetsparken 5, 2100 Copenhagen Ø, Denmark
[c] School of Physics and Astronomy, University of Glasgow, G12 8QQ, UK
[d] Department of Civil and Environmental Engineering, University of Strathclyde, Glasgow, G1 1XJ, UK

ARTICLE INFO

ABSTRACT

Binding of nanoparticles (NPs) to mineral surfaces influences their transport through the environment. The potential, however, for growing minerals to immobilize NPs via occlusion (the process of trapping particles inside the growing mineral) has yet to be explored in environmentally relevant systems. In this study, the ureolytic bacteria *Sporosarcina pasteurii* was used to induce calcium carbonate precipitation in the presence of organo-metallic manufactured nanoparticles. As calcite crystals grew the nanoparticles in the solution became trapped inside these crystals. Capture of NPs within the calcite via occlusion was verified by transmission electron microscopy of thin foils. Nanoparticles with a negative surface charge were captured with greater efficiency than those with a positive surface charge, resulting from stronger attachment of negative nanoparticles to the positively charged calcite surfaces, which in turn facilitated occlusion. Thermodynamic and kinetic analysis, however, did not reveal a significant difference in k_p (calcite precipitation rate constant) or the critical saturation at which precipitation initiates (S_{crit}), indicating the presence of different charged nanoparticles did not influence calcite precipitation at the concentrations used here. Overall, these findings demonstrate that microbially driven mineral precipitation has potential to immobilize nanoparticles in the environment via occlusion.

1. Introduction

Microorganisms have the ability to drive the precipitation of a wide range of minerals. This process can lead to the immobilization of dissolved metals, either within the crystalline structure of the mineral or bound to the mineral surface. For example, microbial oxidation of Fe(II) and Mn(II) generates metal (hydr)oxides which can absorb various dissolved heavy metals and metalloids (Martinez et al., 2004; Pei et al., 2013), while enzymatic precipitation of phosphate produces hydroxyapatite which binds significant quantities of dissolved heavy metals (Handley-Sidhu et al., 2011). Calcite precipitation is common in ground and surface water systems and can be abiotically or biotically driven. A variety of microbial pathways can drive calcite precipitation, including photosynthesis (Merz, 1992), denitrification (van Paassen et al., 2010) and sulphate reduction (Braissant et al., 2007). The capacity to hydrolyse urea (ureolysis) is common in soil and aquifer microorganisms and also has the ability to drive calcite precipitation (Fujita et al., 2010). This process can be manipulated for solid phase capture of heavy metals and radionuclides, where the foreign ion gets incorporated into the calcium carbonate crystal structure as it forms (e.g., ^{90}Sr

replacing Ca in the crystal lattice), thus preventing their mobility in the subsurface (Warren et al., 2001). During ureolysis-driven calcium carbonate precipitation, urea is hydrolysed by the microbial enzyme urease, producing ammonia and carbonic acid (Eq. (1)), which then equilibrates in water to form bicarbonate, ammonium and hydroxide ions. This leads to a pH rise and if soluble calcium is present, an increase in $CaCO_3$ saturation state. Once $CaCO_3$ becomes supersaturated, $CaCO_3$ minerals such as calcite precipitate (Tobler et al., 2011) (Eq. (2)).

$$CO(NH_2)_2 + 2H_2O \leftrightharpoons 2NH_3 + H_2CO_3 \qquad (1)$$

$$Ca^{2+} + HCO_3^- \leftrightharpoons CaCO_3 + H^+ \qquad (2)$$
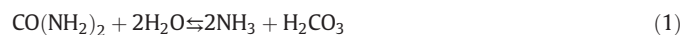
While solid phase capture of dissolved metals during microbial mineral precipitation is a well-known and studied process, the fate of nanometre sized particles during microbial mineral precipitation has not been examined in detail. With a rising demand for nanomaterials and continual growth in production, increased environmental exposure to manufactured nanoparticles (NPs) is likely (Caballero-Guzman and Nowack, 2016). NPs also occur naturally, and both manufactured and natural NPs can act as carriers of heavy metals and organic contaminants (Hofmann and von der Kammer, 2009). To date, investigations into the impact of minerals on nanoparticle transport and fate in the natural environment have largely focused upon the adhesion of

* Corresponding author.
  E-mail address: vernon.phoenix@strath.ac.uk (V.R. Phoenix).

nanoparticles to mineral surfaces (Basnet et al., 2015; Dietrich et al., 2012; Feriancikova and Xu, 2012). However, nanoparticles also have the potential to be immobilized by occlusion (the incorporation of a nanoparticle inside the growing mineral). Thus far however, exploration of how nanoparticles are occluded into minerals has largely been the focus of advanced materials research, where nanoparticles are incorporated to generate synthetic mineral composites with unique properties (Cho et al., 2016; Kim et al., 2010; Kim et al., 2016). As it stands, there is a dearth of information on how occlusion process may impact nanoparticle availability in natural settings. To explore this further, we here utilize a simple, controllable model system – calcite precipitation driven by bacteria. This is relevant as microbial calcite precipitation can occur naturally, but can also be accelerated by stimulation of microbial communities for the purpose of trapping pollutants (Fujita et al., 2010; Mitchell and Ferris, 2005).

In this study, calcite precipitation was driven by the ureolytic bacterium *Sporosarcina pasteurii* (*S. pasteurii*). Experiments were performed as a function of NP surface charge and size to determine if these factors impacted capture efficiency. Capture efficiency was determined by analysing the amount of NPs removed from solution, with capture confirmed by transmission electron microscopy of calcite sections. Thermodynamic and kinetic interpretation of results were undertaken to determine whether these NP properties had a significant impact on precipitation kinetics and the saturation state required for precipitation.

2. Materials and methods

2.1. Nanoparticles

The NPs used in this study exhibit exceptionally high stability, even under high ionic strength, and thus do not aggregate in solution. This is important here as this study aims to demonstrate that NPs can be removed from suspension by occlusion as opposed to aggregation processes. Three different types of NPs were obtained from BioPAL, USA: large negatively charged NP (FeREX, Ø = 150 nm, −38 mV), small negatively charged NP (Molday ION carboxyl terminated, Ø = 35 nm, −38 mV) and small positively charged NPs (Molday ION C6Amine, Ø = 35 nm, +48 mV), They all have a 10 nm nanomagnetite (Fe_3O_4) core surrounded by dextran. Different size and surface charge result from differing thickness of dextran and differing functional groups upon the dextran. This allowed testing the effect of surface charge and particle size on the NP removal efficiency.

Because all NPs types contained identical nanomagnetite cores, Fe was used as a proxy for NP concentration. This enabled NP concentrations to be determined by acid digestion followed by Fe analysis by atomic adsorption spectroscopy (AAS). The initial NP concentration for each experiment was 10 mg $L^{−1}$ Fe. This corresponded to approximately 10^{16} nanoparticles per litre.

2.2. Experimental design

Batch experiments were performed using the gram positive, ureolytic bacterium *S. pasteurii* (strain ATCC 11859). Cultures were grown at 25 °C in brain heart infusion supplemented with filter-sterilised urea (20 g $L^{−1}$). Cells in exponential phase growth were harvested by vacuum filtration (using sterile 0.2 μm membrane filters) and rinsed twice with sterile deionised water (SDW). The bacterial pellet was re-suspended in SDW to an optical density (OD) of 0.14 as determined spectrophotometrically at 600 nm and then pH adjusted to 6.5 using HCl (Analar grade). An OD of 0.14 equates to 2.3×10^6 cells $mL^{−1}$, based on the *S. pasteurii* OD to cell conversion in (Levard et al., 2012). For each nanoparticle immobilization experiment (here-in referred to as NP-I experiment), a solution containing 100 mM $CaCl_2$ and 100 mM urea was prepared and then mixed at a ratio of 1:1 with the bacterial suspension followed by the immediate addition of nanoparticles. The final concentrations were 50 mM $CaCl_2$, 50 mM urea, 10 mg $L^{−1}$

nanoparticles (Fe concentration) and 0.07 OD *S. pasteurii*. During the experiment these batch incubations remained static (i.e. not stirred). In one experiment with l-negNPs, a second injection of 50 mM urea and $CaCl_2$ solution was added into the batch reaction once all initially added urea was converted (using 1 M stock solutions to minimise dilution), to determine if any non-captured NPs could be trapped by a second phase of calcium carbonate precipitation. All nanoparticle immobilization experiments were carried out in triplicate in glass beakers that were covered with *parafilm* to prevent evaporation. Biotic (*S. pasteurii* + urea + NP) and abiotic ($CaCl_2$ + urea + NP) control experiments were also run. In these control experiments, the absence of either bacteria or $CaCl_2$ prevented microbial calcite precipitation, thus revealing if NPs were removed via other mechanisms.

2.3. Chemical analysis

Analyses of solution pH and dissolved NH_4, Ca and Fe were determined at time zero and at regular time intervals thereafter. At each sampling time, 10 mL aliquots were removed from the experiment; 5 mL were used for pH measurement, 0.5 mL to determine NH_4^+ by the Nessler assay and 4.5 mL were mixed with 0.5 mL concentrated HCl for Ca and Fe analyses using atomic absorption spectrometry (AAS, Thermo Scientific iCE 3000 Series). The error for Ca and Fe AAS measurements as determined from repeated measurements of the same sample was within analytical uncertainty (≤5%).

2.4. Transmission electron microscopy (TEM)

TEM imaging, selected area electron diffraction (SAED) and energy-dispersive X-ray spectroscopy (EDXS) were undertaken on thin foils that were prepared from calcite grains using the Focused Ion Beam (FIB) lift-out technique with a FEI Nova 200 Dualbeam. Calcite crystal surfaces were first sputter coated with gold to prevent charging of the mineral surface and ion-implantation into the calcite, followed by further deposition of platinum from an organometallic precursor within the FIB. Foils were thinned using a 30 kV Ga^+ ion beam to a thickness of ~1 μm prior to being removed from their parent grain using an in-situ micromanipulator. Foils were welded to the tines of an Omniprobe copper support using electron and ion beam deposited platinum. Final thinning was performed using lower accelerating voltages and beam currents on these supported thin foils to reduce the total thickness to less than ~60 nm in the thinnest areas in order to facilitate EELS (Electron Energy Loss Spectroscopy), without compromising the crystallinity. Initial characterisation of these foils by diffraction-contrast imaging and SAED was performed using a FEI T20 TEM operated at 200 kV. EELS analysis was performed using a JEOL ARM200F equipped with a Gatan GIF Quantum Electron Energy Loss Spectrometer; the EELS work was undertaken at an accelerating voltage of 80 kV in scanning TEM (STEM) mode using line scans with a nominal step size of about 1 nm.

2.5. Kinetic analysis of calcite precipitation

To determine if the presence of NPs and their properties (size and surface charge) affected $CaCO_3$ precipitation rates (e.g., through NPs acting as nucleation sites and/or growth inhibitors), we determined calcite precipitation kinetics as described in Tobler et al. (2011). See supplemental information for details of calculations. In summary, the rate constant for calcite precipitation (k_p) and the critical saturation at which precipitation initiates (S_{crit}), can be determined from the following first order reaction (Tobler et al., 2011).

$$\left[Ca^{2+}\right] = \left(\frac{k_p}{k_s}\right)\left[S - S_{crit} - \ln\left(\frac{S}{S_{crit}}\right)\right] + \left[Ca^{2+}\right]_{crit} \qquad (3)$$

where $[Ca^{2+}]_{crit}$ is the dissolved Ca concentration at S_{crit} and k_s is a first